

# Enzyme-Responsive Aqueous Two-Phase Systems in a Cationic–Anionic Surfactant Mixture

Xiao Xiao, Yan Qiao, Zhirui Xu, Tongyue Wu, Yunxue Wu, Zhe Ling, Yun Yan, and Jianbin Huang\*



Cite This: <https://doi.org/10.1021/acs.langmuir.1c02303>



Read Online

ACCESS |



Metrics & More

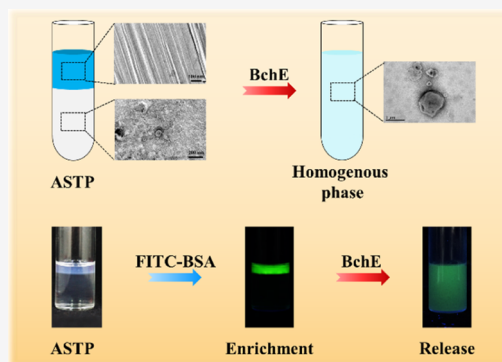


Article Recommendations



Supporting Information

**ABSTRACT:** Enzyme-instructed self-assembly is an increasingly attractive topic owing to its broad applications in biomaterials and biomedicine. In this work, we report an approach to construct enzyme-responsive aqueous surfactant two-phase (ASTP) systems serving as enzyme substrates by using a cationic surfactant (myristoylcholine chloride) and a series of anionic surfactants. Driven by the hydrophobic interaction and electrostatic attraction, self-assemblies of cationic–anionic surfactant mixtures result in biphasic systems containing condensed lamellar structures and coexisting dilute solutions, which turn into homogeneous aqueous phases in the presence of hydrolase (cholinesterase). The enzyme-sensitive ASTP systems reported in this work highlight potential applications in the active control of biomolecular enrichment/release and visual detection of cholinesterase.



## INTRODUCTION

Enzyme-responsive systems are attractive research areas owing to the potential applications in broad fields including drug delivery,<sup>1–4</sup> tumor imaging,<sup>5–9</sup> bio-inspired assemblies,<sup>10–12</sup> and biological materials.<sup>13–15</sup> For example, enzymatic hydrogelation formed by polymers<sup>16–20</sup> or small molecules has been utilized in enzyme inhibitor screening,<sup>21–24</sup> cancer therapy,<sup>6,25</sup> and tissue engineering.<sup>26,27</sup> However, the enzyme-responsive aqueous two-phase system has been an attractive system for biological material processing due to its gentle high water content environments.<sup>28–31</sup> The aqueous two-phase system is a phase separation phenomenon that was observed in polymer solutions initially.<sup>32–35</sup> Subsequently, a similar phenomenon termed as aqueous surfactant two-phases (ASTP) was demonstrated with aqueous mixtures of cationic–anionic surfactants.<sup>36–40</sup> In an ASTP system, the solution separates spontaneously into two immiscible aqueous phases with a clear interfacial boundary between them, where one phase is rich in surfactants and the other one is the dilute phase. The spontaneous formation of a highly concentrated surfactant solution has enabled the selective concentration of biomolecules,<sup>41,42</sup> carbon tubes,<sup>43,44</sup> metal ions,<sup>45</sup> and small molecules.<sup>46</sup> We envision that the coupling of ASTP with external stimuli-responsiveness will allow for active separation of a variety of biomolecules or biomaterials. Compared to other stimuli, enzymes have advantages in terms of specificity and efficiency in triggering chemical reactions and thereby amplifying changes beyond molecular scales (e.g., supramolecular properties). Because secretory enzymes are closely related to biological activities and their abnormal expression is often associated with the development of human diseases, the

exploration of enzyme-responsive ASTP is also of great significance in the fields of clinical medicine.

In this work, we reported enzyme-responsive ASTP systems formed by the mixture of myristoylcholine chloride (MChCl) and a series of anionic surfactants such as sodium laurate (SL), sodium octyl sulfonate (SOS), and sodium decanoate (SD). It is known that the association of the oppositely charged surfactant can form ASTP under certain conditions (e.g., concentration, pH, temperature, and mixing ratio). The electrostatic interaction between cationic and anionic surfactants is an essential factor for the formation of ASTP,<sup>37,47</sup> where the variation of charges results in microstructural transition associated with macroscopic phase behavior of surfactant systems. This inspired us to design enzyme-responsive aqueous phase behaviors from cationic–anionic surfactants, in which the positive/negative charge ratio of surfactants can be adjusted by enzymatic hydrolysis of surfactants.

To this goal, MChCl was employed as the cationic surfactant and the enzyme substrate that can be converted to myristic acid and choline in the presence of cholinesterases. Electrostatic interactions between myristoylcholine and anionic surfactants lead to the formation of ASTP. With the response to cholinesterase, the cationic–anionic ASTP can be eventually

Received: August 30, 2021

Revised: October 10, 2021

turned into a single homogeneous aqueous phase accompanied with cationic surfactant MChCl converted into anionic myristic acid. We anticipate that the cholinesterase-sensitive ASTP can serve as a potential platform for active separation of biomolecules and the visual detection of cholinesterase.

## EXPERIMENTAL SECTION

**Materials.** MChCl (99%) was purchased from TRC. SL (98%) and SD (98%) were purchased from Aladdin. SOS (98%) was purchased from Macklin. Butyryl cholinesterase (BchE) and deuterium oxide ( $D_2O$ , 99%) were purchased from Sigma. Nile red was purchased from TCI. Fluorescein isothiocyanate-bovine serum albumin (FITC-BSA) was provided by Prof. Yan Qiao group, Institute of Chemistry, Chinese Academy of Sciences. Aqueous solutions were prepared using Milli-Q water of 18  $M\Omega$ .

**Sample Preparation.** Samples were prepared by mixing the stock solutions of cationic and anionic surfactants at a desired concentration and mixing ratio at 25 °C. Samples were vortically mixed after sealing. Unless specifically stated, the pH of MChCl and the anionic surfactant mixed system was fixed to 7.2 (Tris-HCl).

**$^1H$  Nuclear Magnetic Resonance.** The  $^1H$  nuclear magnetic resonance ( $^1H$  NMR) experiments were performed on a Bruker ARX 500 MHz spectrometer with  $D_2O$  as a solvent at 25 °C.

**Transmission Electron Microscopy.** Samples were prepared by the negative-staining method (with uranyl acetate) and freeze fracture replication technique and then observed by Tecnai T20 (200 kV). For the negative-staining method, a drop of the sample was added onto a 200 mesh copper grid coated with the Formvar film. Excess solution was removed with a piece of filter paper, and the samples were stained with 3% uranyl acetate for 3–5 min. The excess staining agent was removed with filter papers before transmission electron microscopy (TEM) observation. Also, the freeze fracture replication technique was carried out in a high-vacuum freeze-etching system (Balzers BAF-400D).

**Electrospray Ionization Mass Spectrometry.** Electrospray ionization mass spectrometry (ESI-MS) measurements were carried out on an APEX IV FT-MS (Bruker). The operating condition of the ESI source was in negative ion mode.

**Rheology.** The rheological properties of the samples were measured at 25 °C with a Thermo Haake RS300 rheometer (cone and plate geometry of 35 mm in diameter with the cone gap equal to 0.105 mm).

**Elemental Analysis.** The elemental analyses were carried out on a Vario EL elemental analyzer (Elementar Analysensysteme GmbH, Langensfeld, Germany).

**Fluorescence Spectrometry.** Fluorescence spectra were recorded on a Hitachi F7000 spectrometer equipped with a constant temperature bath to control the temperature at 25 °C ( $\lambda_{ex} = 540$  nm).

## RESULTS AND DISCUSSION

**Phase Behavior and Microstructures of MChCl/SL Mixed System.** Mixtures of MChCl and SL were prepared by mixing the stock solutions at different total concentrations ( $c_{total}$ ,  $c_t$ ) and mixing ratios ( $x_{SL}$ ). The phase diagram of MChCl/SL mixed systems is shown in Figure 1a at pH 7.2, in which the homogenous phase, ASTP, and precipitate were observed when  $c_t$  was higher than 10 mM (illustrated in Figure 1b). At the total concentration of 40 mM (Figure 1c), it was observed that when cationic surfactant MChCl dominated ( $x_{SL} < 0.25$ ), the solutions remained homogenous and clear with vesicles inside (Figure S1). With the increase of  $x_{SL}$ , ASTP of two coexisting phases was observed ( $0.25 < x_{SL} < 0.4$ ) and the heterogeneous mixture emerged ( $0.45 < x_{SL} < 0.55$ ). The turbidity confirmed the macroscopic phenomena in the two phases of ASTP and homogenous solutions (Figure S2). The high value of  $x_{SL}$  ( $0.6 < x_{SL}$ ) would result in the homogenous solution with the vesicles inside (Figure S1). Moreover, ASTP

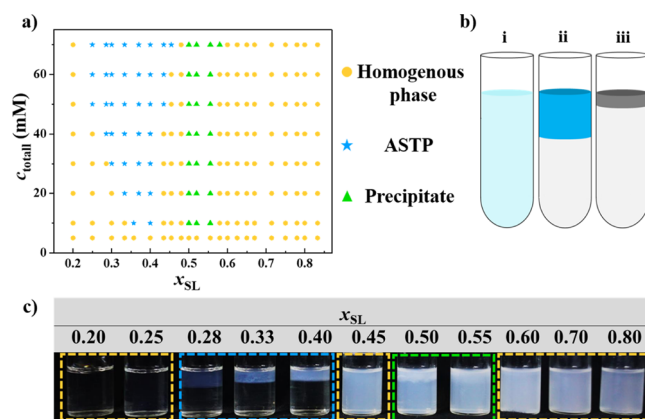


**Figure 1.** (a) Phase diagram for MChCl/SL mixed systems at pH = 7.2. (b) Schematic illustration of the three types of phase behaviors in MChCl/SL mixed systems: (i) homogenous solution, (ii) ASTP, and (iii) precipitate and solution. (c) Photographs of MChCl/SL mixed systems at different mixing ratios ( $c_t = 40$  mM, pH = 7.2).

can remain stable at 25–40 °C or with NaCl up to 20 mM (Figure S3).

Figure 2a shows the macroscopic appearance of the ASTP system ( $c_t = 40$  mM,  $x_{SL} = 0.40$ , pH = 7.2, 25 °C), in which the volume ratio of the upper to lower phase is about 1:3, and the upper phase was opalescent with a slightly bluish. Under two polarizers, the upper phase displayed birefringence (ii), while the lower phase was clear without any birefringence. The upper phase was demonstrated to show higher capacity to solubilize hydrophobic dye oil red than the lower phase (iii). In addition, the upper phase was shown to be viscous with a shear-thinning effect (Figure 2b), while the lower phase displayed water-like fluid behavior. Structurally, the birefringence of the upper phase indicated the existence of lamellar structures, which can be confirmed by freeze-fracture TEM (FF-TEM) (Figure 2c). The ordered structure was further confirmed by X-ray diffraction (XRD) shown in Figure 2e, where three Bragg diffraction peaks correspond to distances of 41.8, 21.1, and 14.0 Å and these peaks indicated the presence of lamellar structures.<sup>48</sup> The thickness of the lamellae was determined from the 001 diffraction peak to be 41.8 Å, that is, approximately the sum of the length of extended MChCl and SL molecules (Figure 2f). The fluorescence spectroscopy also confirmed that the molecular arrangement is more orderly in the lamellar phase (Figure S4). In contrast, the formation of spherical vesicles in the lower phase of ASTP and other homogenous solutions was demonstrated by negative-stained TEM (Figure 2d). It is therefore concluded that lamellar structures exist in the surfactant-rich upper phase, while vesicles exist in the bottom phase with low surfactant concentration. Elemental analysis (Table S1) and NMR (Figure S5) confirmed the results that the upper phase is the surfactant-enriched one, while the lower phase is a very dilute phase.

**Enzyme Response of ASTP Systems.** MChCl can be hydrolyzed by cholinesterase into myristate and choline, leading to enzyme-responsive ASTP system. To demonstrate this, 10 U/mL BchE was added into the ASTP system ( $c_t = 12$  mM,  $x_{SL} = 0.40$ ) and incubated at 25 °C. The hydrolysis of MChCl and the production of choline were tracked by  $^1H$  NMR. Figure 3a illustrates the enzymatic reaction of MChCl in the presence of BchE. After the enzymatic reaction for 24 h, the

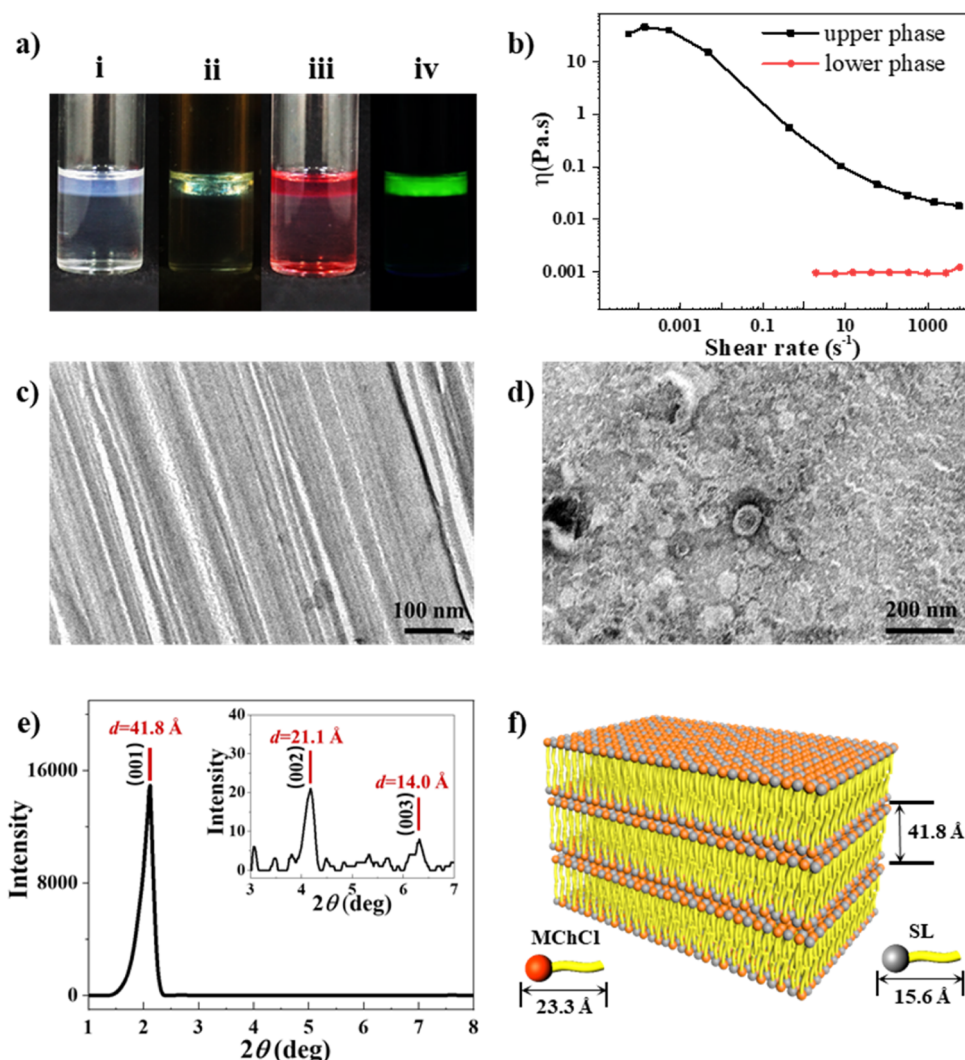


**Figure 2.** (a) Macroscopic appearance for MChCl/SL ASTP ( $c_t = 20 \text{ mM}$ ,  $x_{SL} = 0.40$ ): (i) under visible light, (ii) under the polarizer, (iii) with the addition of hydrophobic dye oil red, and (iv) with the addition of 0.1 mg/mL FITC-BSA and under the UV light. (b) Steady rheology results of upper and bottom phases for MChCl/SL ASTP ( $c_t = 40 \text{ mM}$ ,  $x_{SL} = 0.40$ ). (c) FF-TEM image for the upper phase of ASTP. (d) Negative-stained TEM image for the lower phase of ASTP. (e) XRD result for the upper phase of ASTP. (f) Schematic illustration of the lamellar structure in the upper phase.

ASTP system disappeared and the two phases turned to be homogenous (Figure 3b), with a lower viscosity than the upper phase of the ASTP system (Figure S6). Negative-stained TEM observation confirmed that no lamellae existed in the system but the thick-walled vesicles (Figure 3c). The presence of BchE converted MChCl into an anionic surfactant myristic acid. As a result, electrostatic attractions between cationic–anionic surfactants to form ASTP (lamellar structure in the upper phase and vesicles in the lower phase) were replaced by repulsive force, causing the transition to a single homogeneous phase with thick-walled vesicles inside. Figure 3d shows that the feature peaks of choline are produced gradually. ESI–MS analysis confirmed that the molecular structure of SL did not change during the enzymatic process (Figure S7). The enzyme reaction is affected by pH<sup>49</sup> and temperature,<sup>50,51</sup> and generally, the enzyme activity is highest at 25–37 °C. The appropriate pH depends on the properties of the enzyme itself. Considering the characteristics of the ASTP, pH = 7.2 and 25 °C were chosen as the reaction conditions of the enzyme. In addition, the turnover number of BchE is about 4796 min<sup>-1</sup>.

### Universality of the Enzyme-Responsive ASTP System.

The MChCl/SL ASTP system showed the specific response to BchE, while no sensitivity to other enzymes, such as  $\alpha$ -amylase (Figure S8). Moreover, replacing SL with other amphiphiles could also construct the ASTP systems with MChCl. Figure 4a shows the phase diagram of MChCl/SOS at pH 7.2, and the phase situations are illustrated in Figure 4b ( $c_t = 40 \text{ mM}$ ). Different from the MChCl/SL ASTP system, the upper phase of MChCl/SOS ASTP had no birefringence, indicating that there may be no lamellar structure. Figure 4c,d shows the microstructures in the upper phase and lower phase by negative-stained TEM, respectively, where fused vesicles were in the surfactant-rich upper phase, which was also verified by the viscosity measurements (Figure S9). The enzyme-responsiveness for the ASTP system is shown in Figure S10, and the precipitates formed after the BchE reaction and optical microscopy image showed the microstructure turned to be flakes. ESI–MS confirmed that the SOS had no change during enzyme reaction (Figure S11). The macroscopical appearance

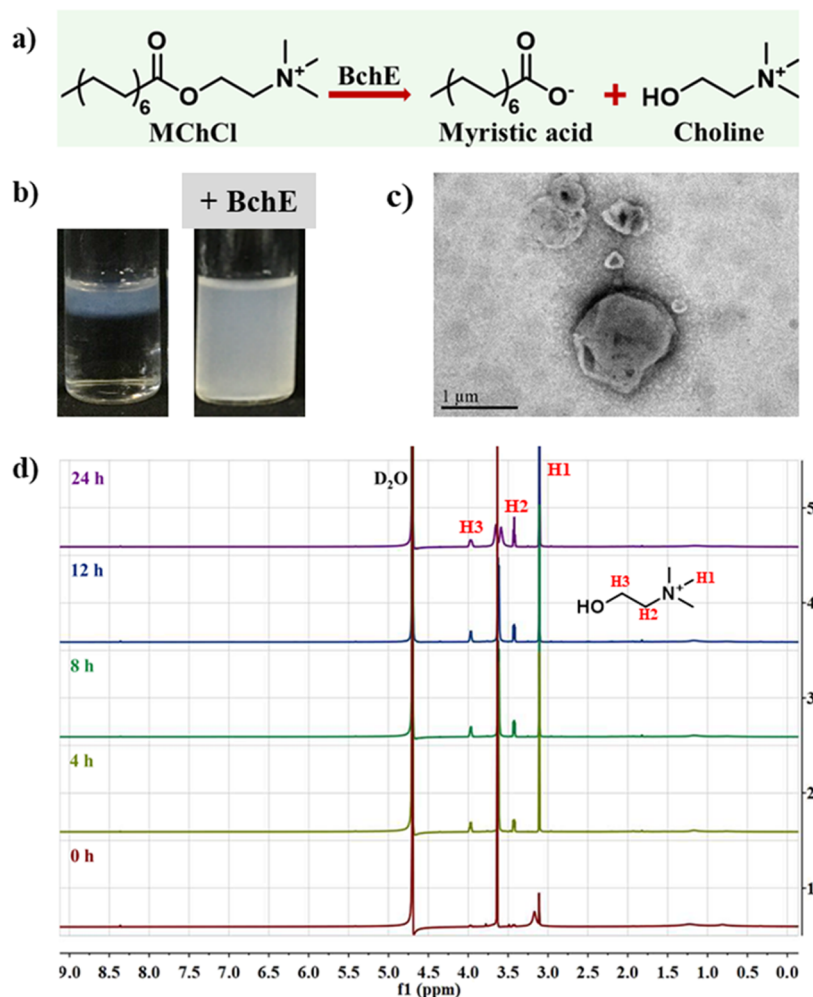


**Figure 3.** (a) Enzymatic reaction of MChCl in the presence of BchE. (b) Photographs of the MChCl/SL ASTP ( $c_t = 12$  mM,  $x_{\text{SL}} = 0.40$ ) before and after 10 U/mL BchE reaction. (c) Negative-stained TEM image for the MChCl/SL ASTP system after the enzyme reaction. (d)  $^1\text{H}$  NMR spectra for MChCl/SL ASTP during 10 U/mL BchE reaction.

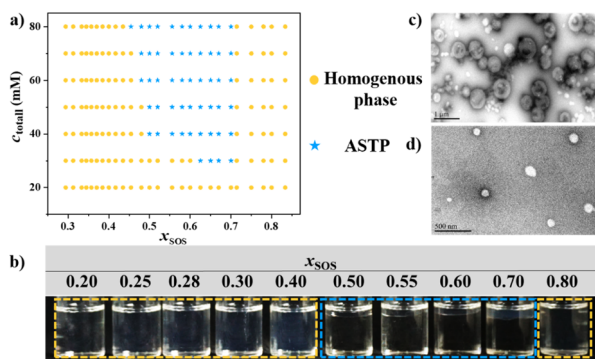


**Figure 4.** (a) Phase diagram for MChCl/SOS mixed systems at pH 7.2. (b) Photographs of MChCl/SOS mixed systems ( $c_t = 40$  mM). Negative-stained TEM images for the ASTP system: (c) upper phase and (d) lower phase.

and properties in MChCl/SD mixed systems and their enzyme response of ASTP are shown in Figure S12.

**Visual Detection for Cholinesterase and Active Enrichment/Release of Biomolecules in ASTP System.** The visible macroscopic phase transition from ASTP to a homogeneous solution or precipitate by the addition of BchE can be potentially utilized to detect cholinesterase, which is key

to daily metabolism and the overexpression may lead to diseases. The ASTP formed by MChCl/SL mixing ( $c_t = 10$  mM,  $x_{\text{SL}} = 0.40$ ) was used for concept-proof, in which the original system exhibited two co-existing solutions. As shown in Figure 5a, the upper phase was opalescent and the bottom phase was transparent. With the addition of 5 U/mL BchE, the phenomenon of ASTP disappeared. We therefore envisioned

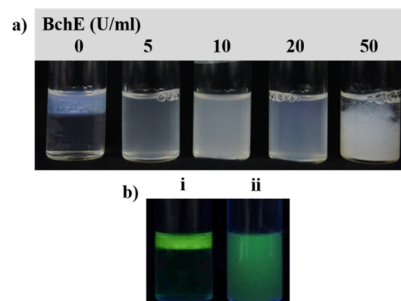


**Figure 5.** (a) Macroscopic photographs of MChCl/SL ASTP systems ( $c_t = 10$  mM,  $x_{\text{SL}} = 0.40$ ) with 0, 5, 10, 20, and 50 U/mL of BchE. (b) Macroscopic photographs of MChCl/SL ASTP systems with the addition of FITC-BSA before (i) and after (ii) adding 10 U/mL of BchE under the UV light.

that this ASTP system can be utilized as a potential tool for naked-eye detection of enzymes. Figure 5b shows the ability of enrichment for biomolecules of the ASTP system. 0.1 mg/mL FITC-BSA was added into the ASTP system ( $c_t = 20$  mM,  $x_{SL} = 0.40$ ), and under the UV light, the upper phase displayed green fluorescence, while the lower phase was dark (i). After adding 10 U/mL of BchE, the whole solution displayed fluorescence (ii), which confirmed that the ASTP turned to be homogenous after the BchE reaction and the FITC-BSA released into the solution.

## CONCLUSIONS

In conclusion, we herein report an approach to construct enzyme-responsive ASTP systems with BchE-cleavable cationic surfactant MChCl and enzyme-insert anionic surfactants (e.g., SL, SOS, and SD). Depending on the cationic–anionic ratio, the surfactant mixture was found to aggregate into a variety of nanostructures, accompanied by the emergence of macroscopic phase separation. The presence of BchE was found to trigger the hydrolysis of ester bonds, converting MChCl into an anionic surfactant myristic acid. As a result, electrostatic attractions between cationic–anionic surfactants (MChCl/SOS, MChCl/SL, and MChCl/SD) were replaced by repulsive force, causing the dissociation of high-ordered self-assembly. We anticipate that this work represents a facile approach to design biologically active soft materials across different scales, which will find potential applications in broad fields such as smart delivery and biosensing.

## ASSOCIATED CONTENT

### Supporting Information

The Supporting Information is available free of charge at <https://pubs.acs.org/doi/10.1021/acs.langmuir.1c02303>.

Materials, negative-stain TEM images, ESI–MS results, macroscopic photographs, and steady shear results (PDF)

## AUTHOR INFORMATION

### Corresponding Author

**Jianbin Huang** – Beijing National Laboratory for Molecular Sciences (BNLMS), State Key Laboratory for Structural Chemistry of Unstable and Stable Species, College of Chemistry and Molecular Engineering, Peking University, Beijing 100871, P. R. China; Email: [jbhuang@pku.edu.cn](mailto:jbhuang@pku.edu.cn)

### Authors

**Xiao Xiao** – Beijing National Laboratory for Molecular Sciences (BNLMS), State Key Laboratory for Structural Chemistry of Unstable and Stable Species, College of Chemistry and Molecular Engineering, Peking University, Beijing 100871, P. R. China; [orcid.org/0000-0003-3216-9110](https://orcid.org/0000-0003-3216-9110)

**Yan Qiao** – Beijing National Laboratory for Molecular Sciences, State Key Laboratory of Polymer Physics and Chemistry, CAS Research/Education Center for Excellence in Molecular Sciences, Institute of Chemistry, Chinese Academy of Sciences, Beijing 100190, P. R. China; [orcid.org/0000-0003-1069-7756](https://orcid.org/0000-0003-1069-7756)

**Zhirui Xu** – Beijing National Laboratory for Molecular Sciences (BNLMS), State Key Laboratory for Structural Chemistry of Unstable and Stable Species, College of

Chemistry and Molecular Engineering, Peking University, Beijing 100871, P. R. China

**Tongyue Wu** – Beijing National Laboratory for Molecular Sciences (BNLMS), State Key Laboratory for Structural Chemistry of Unstable and Stable Species, College of Chemistry and Molecular Engineering, Peking University, Beijing 100871, P. R. China

**Yunxue Wu** – Beijing National Laboratory for Molecular Sciences (BNLMS), State Key Laboratory for Structural Chemistry of Unstable and Stable Species, College of Chemistry and Molecular Engineering, Peking University, Beijing 100871, P. R. China

**Zhe Ling** – Jiangsu Co-Innovation Center of Efficient Processing and Utilization of Forest Resources, College of Chemical Engineering, Nanjing Forestry University, Nanjing 210037, P. R. China; [orcid.org/0000-0002-1702-8267](https://orcid.org/0000-0002-1702-8267)

**Yun Yan** – Beijing National Laboratory for Molecular Sciences (BNLMS), State Key Laboratory for Structural Chemistry of Unstable and Stable Species, College of Chemistry and Molecular Engineering, Peking University, Beijing 100871, P. R. China; [orcid.org/0000-0001-8759-3918](https://orcid.org/0000-0001-8759-3918)

Complete contact information is available at: <https://pubs.acs.org/10.1021/acs.langmuir.1c02303>

### Author Contributions

The manuscript was written through contributions of all authors. All authors have given approval to the final version of the manuscript.

### Notes

The authors declare no competing financial interest.

## ACKNOWLEDGMENTS

This work is supported by the National Natural Science Foundation of China (NSFC, grant nos. 21972003 and 21633002).

## REFERENCES

- (1) de la Rica, R.; Aili, D.; Stevens, M. M. Enzyme-Responsive Nanoparticles for Drug Release and Diagnostics. *Adv. Drug Delivery Rev.* **2012**, *64*, 967–978.
- (2) Gehlot, P. S.; Rao, K. S.; Bharmoria, P.; Damarla, K.; Gupta, H.; Drechsler, M.; Kumar, A. Spontaneous Formation of Multi-architecture Vesicles of  $[C_{8mim}]Br^+$   $[Na]DBS$  in Aqueous Medium: Synergic Interplay of Electrostatic, Hydrophobic, and  $\pi$ - $\pi$  Stacking Interactions. *J. Phys. Chem. B* **2015**, *119*, 15300–15309.
- (3) Oh, S. S.; Lee, B. F.; Leibfarth, F. A.; Eisenstein, M.; Robb, M. J.; Lynd, N. A.; Hawker, C. J.; Soh, H. T. Synthetic Aptamer-Polymer Hybrid Constructs for Programmed Drug Delivery into Specific Target Cells. *J. Am. Chem. Soc.* **2014**, *136*, 15010–15015.
- (4) Blum, A. P.; Kammeyer, J. K.; Rush, A. M.; Callmann, C. E.; Hahn, M. E.; Gianneschi, N. C. Stimuli-Responsive Nanomaterials for Biomedical Applications. *J. Am. Chem. Soc.* **2015**, *137*, 2140–2154.
- (5) Li, X.; Wang, Y.; Yang, C.; Shi, S.; Jin, L.; Luo, Z.; Yu, J.; Zhang, Z.; Yang, Z.; Chen, H. Supramolecular Nanofibers of Triamcinolone Acetonide for Uveitis Therapy. *Nanoscale* **2014**, *6*, 14488–14494.
- (6) Zhou, J.; Xu, B. Enzyme-Instructed Self-Assembly: A Multistep Process for Potential Cancer Therapy. *Bioconjugate Chem.* **2015**, *26*, 987–999.
- (7) Tong, H.; Du, J.; Li, H.; Jin, Q.; Wang, Y.; Ji, J. Programmed Photosensitizer Conjugated Supramolecular Nanocarriers with Dual Targeting Ability for Enhanced Photodynamic Therapy. *Chem. Commun.* **2016**, *52*, 11935–11938.
- (8) Wu, C.; Zhang, R.; Du, W.; Cheng, L.; Liang, G. Alkaline Phosphatase-Triggered Self-Assembly of Near-Infrared Nanoparticles

- for the Enhanced Photoacoustic Imaging of Tumors. *Nano Lett.* **2018**, *18*, 7749–7754.
- (9) Gao, Y.; Shi, J.; Yuan, D.; Xu, B. Imaging Enzyme-Triggered Self-Assembly of Small Molecules inside Live Cells. *Nat. Commun.* **2012**, *3*, 1033.
- (10) Wang, H.; Feng, Z.; Xu, B. Bioinspired Assembly of Small Molecules in Cell Milieu. *Chem. Soc. Rev.* **2017**, *46*, 2421–2436.
- (11) Feng, Z.; Wang, H.; Xu, B. Instructed Assembly of Peptides for Intracellular Enzyme Sequestration. *J. Am. Chem. Soc.* **2018**, *140*, 16433–16437.
- (12) Kuang, Y.; Shi, J.; Li, J.; Yuan, D.; Alberti, K. A.; Xu, Q.; Xu, B. Pericellular Hydrogel/Nanonets Inhibit Cancer Cells. *Angew. Chem., Int. Ed.* **2014**, *53*, 8104–8107.
- (13) Lu, Y.; Aimetti, A. A.; Langer, R.; Gu, Z. Bioresponsive Materials. *Nat. Rev. Mater.* **2017**, *2*, 16075.
- (14) Li, J.; Maniar, D.; Qu, X.; Liu, H.; Tsao, C.-Y.; Kim, E.; Bentley, W. E.; Liu, C.; Payne, G. F. Coupling Self-Assembly Mechanisms to Fabricate Molecularly and Electrically Responsive Films. *Biomacromolecules* **2019**, *20*, 969–978.
- (15) Ooya, T.; Eguchi, M.; Yui, N. Enhanced Accessibility of Peptide Substrate toward Membrane-Bound Metalloexopeptidase by Supramolecular Structure of Polyrotaxane. *Biomacromolecules* **2001**, *2*, 200–203.
- (16) Sperinde, J. J.; Griffith, L. G. Synthesis and Characterization of Enzymatically-Cross-Linked Poly(Ethylene Glycol) Hydrogels. *Macromolecules* **1997**, *30*, 5255–5264.
- (17) Hu, B.-H.; Messersmith, P. B. Rational Design of Transglutaminase Substrate Peptides for Rapid Enzymatic Formation of Hydrogels. *J. Am. Chem. Soc.* **2003**, *125*, 14298–14299.
- (18) Sanborn, T. J.; Messersmith, P. B.; Barron, A. E. In Situ Crosslinking of a Biomimetic Peptide-PEG Hydrogel via Thermally Triggered Activation of Factor XIII. *Biomaterials* **2002**, *23*, 2703–2710.
- (19) Lutolf, M. P.; Raeber, G. P.; Zisch, A. H.; Tirelli, N.; Hubbell, J. A. Cell-Responsive Synthetic Hydrogels. *Adv. Mater.* **2003**, *15*, 888–892.
- (20) Sharma, K. P.; Harniman, R.; Farrugia, T.; Briscoe, W. H.; Perriman, A. W.; Mann, S. Dynamic Behavior in Enzyme-Polymer Surfactant Hydrogel Films. *Adv. Mater.* **2016**, *28*, 1597–1602.
- (21) Yang, Z.; Liang, G.; Xu, B. Enzymatic Hydrogelation of Small Molecules. *Acc. Chem. Res.* **2008**, *41*, 315–326.
- (22) Hughes, M.; Frederix, P. W. J. M.; Raeburn, J.; Birchall, L. S.; Sadownik, J.; Coomer, F. C.; Lin, I.-H.; Cussen, E. J.; Hunt, N. T.; Tuttle, T.; Webb, S. J.; Adams, D. J.; Ulijn, R. V. Sequence/Structure Relationships in Aromatic Dipeptide Hydrogels Formed under Thermodynamic Control by Enzyme-Assisted Self-Assembly. *Soft Matter* **2012**, *8*, 5595–5602.
- (23) Yang, Z.; Liang, G.; Wang, L.; Xu, B. Using a Kinase/Phosphatase Switch to Regulate a Supramolecular Hydrogel and Forming the Supramolecular Hydrogel in Vivo. *J. Am. Chem. Soc.* **2006**, *128*, 3038–3043.
- (24) Yang, Z.; Gu, H.; Fu, D.; Gao, P.; Lam, J. K.; Xu, B. Enzymatic Formation of Supramolecular Hydrogels. *Adv. Mater.* **2004**, *16*, 1440–1444.
- (25) Van Bommel, K. J. C.; Stuart, M. C. A.; Feringa, B. L.; Van Esch, J. Two-Stage Enzyme Mediated Drug Release from LMWG Hydrogels. *Org. Biomol. Chem.* **2005**, *3*, 2917–2920.
- (26) Nguyen, M. M.; Carlini, A. S.; Chien, M.-P.; Sonnenberg, S.; Luo, C.; Braden, R. L.; Osborn, K. G.; Li, Y.; Gianneschi, N. C.; Christman, K. L. Enzyme-Responsive Nanoparticles for Targeted Accumulation and Prolonged Retention in Heart Tissue after Myocardial Infarction. *Adv. Mater.* **2015**, *27*, 5547–5552.
- (27) Jayawarna, V.; Ali, M.; Jowitt, T. A.; Miller, A. F.; Saiani, A.; Gough, J. E.; Ulijn, R. V. Nanostructured Hydrogels for Three-Dimensional Cell Culture through Self-Assembly of Fluorenylmethoxycarbonyl-Dipeptides. *Adv. Mater.* **2006**, *18*, 611–614.
- (28) Yu, M.; Liu, Z.; Du, Y.; Ma, C.; Yan, Y.; Huang, J. Endowing a Light-Inert Aqueous Surfactant Two-Phase System with Photoresponsiveness by Introducing a Trojan Horse. *ACS Appl. Mater. Interfaces* **2019**, *11*, 15103–15110.
- (29) Kim, B. S.-I.; Jin, Y.-J.; Sakaguchi, T.; Lee, W.-E.; Kwak, G. Fluorescence Response of Conjugated Polyelectrolyte in an Immiscible Two-Phase System via Nonelectrostatic Interaction with Surfactants. *ACS Appl. Mater. Interfaces* **2015**, *7*, 13701–13706.
- (30) Martin, N.; Tian, L.; Spencer, D.; Coutable-Pennarun, A.; Anderson, J. L. R.; Mann, S. Photoswitchable Phase Separation and Oligonucleotide Trafficking in DNA Coacervate Microdroplets. *Angew. Chem., Int. Ed.* **2019**, *58*, 14594–14598.
- (31) Cacace, D. N.; Keating, C. D. Biocatalyzed Mineralization in an Aqueous Two-Phase System: Effect of Background Polymers and Enzyme Partitioning. *J. Mater. Chem. B* **2013**, *1*, 1794–1803.
- (32) Torres-Acosta, M. A.; Mayolo-Deloiisa, K.; González-Valdez, J.; Rito-Palomares, M. Aqueous Two-Phase Systems at Large Scale: Challenges and Opportunities. *Biotechnol. J.* **2019**, *14*, No. e1800117.
- (33) Posharnowa, N.; Schneider, A.; Wunsch, M.; Kuleznev, V.; Wolf, B. A. Polymer-Polymer Interaction Parameters for Homopolymers and Copolymers from Light Scattering and Phase Separation Experiments in a Common Solvent. *J. Chem. Phys.* **2001**, *115*, 9536–9546.
- (34) Hatti-Kaul, R. Aqueous Two-Phase Systems: A General Overview. *Mol. Biotechnol.* **2001**, *19*, 269–278.
- (35) Lee, J. H.; Lee, J. K.; Lee, K. H.; Lee, C. H. Phase Separation and Crystallization Behavior in Extruded Polypropylene/Ethylene-Propylene Rubber Blends Containing Ethylene-Olefin Copolymers. *Polym. J.* **2000**, *32*, 321–325.
- (36) Yu, Z.-J.; Zhao, G.-X. The Physicochemical Properties of Aqueous Mixtures of Cationic-Anionic Surfactants: I. *J. Colloid Interface Sci.* **1989**, *130*, 414–420.
- (37) Yin, H.; Mao, M.; Huang, J.; Fu, H. Two-Phase Region in the DTAB/SL Mixed Surfactant System. *Langmuir* **2002**, *18*, 9198–9203.
- (38) Zhao, G.-X.; Xiao, J.-X. Aqueous Two-Phase Systems of the Aqueous Mixtures of Cationic-Anionic Surfactants. *J. Colloid Interface Sci.* **1996**, *177*, 513–518.
- (39) Lu, T.; Li, Z.; Huang, J.; Fu, H. Aqueous Surfactant Two-Phase Systems in a Mixture of Cationic Gemini and Anionic Surfactants. *Langmuir* **2008**, *24*, 10723–10728.
- (40) Yu, Z.-J.; Zhao, G.-X. The Physicochemical Properties of Aqueous Mixtures of Cationic-Anionic Surfactants. II. Micelle Growth Pattern of Equimolar Mixtures. *J. Colloid Interface Sci.* **1989**, *130*, 421–431.
- (41) Xiao, J. X.; Sivars, U.; Tjerneld, F. Phase Behavior and Protein Partitioning in Aqueous Two-Phase Systems of Cationic-Anionic Surfactant Mixtures. *J. Chromatogr. B: Biomed. Sci. Appl.* **2000**, *743*, 327–338.
- (42) Vijayakumar, K.; Gulati, S.; Demello, A. J.; Edel, J. B. Rapid Cell Extraction in Aqueous Two-Phase Microdroplet Systems. *Chem. Sci.* **2010**, *1*, 447–452.
- (43) Fagan, J. A.; Huh, J. Y.; Simpson, J. R.; Blackburn, J. L.; Holt, J. M.; Larsen, B. A.; Walker, A. R. H. Separation of Empty and Water-Filled Single-Wall Carbon Nanotubes. *ACS Nano* **2011**, *5*, 3943–3953.
- (44) Fagan, J. A.; Hároz, E. H.; Ihly, R.; Gui, H.; Blackburn, J. L.; Simpson, J. R.; Lam, S.; Hight Walker, A. R.; Doorn, S. K.; Zheng, M. Isolation of >1 Nm Diameter Single-Wall Carbon Nanotube Species Using Aqueous Two-Phase Extraction. *ACS Nano* **2015**, *9*, 5377–5390.
- (45) Akama, Y.; Ito, M.; Tanaka, S. Selective Separation of Cadmium from Cobalt, Copper, Iron (III) and Zinc by Water-Based Two-Phase System of Tetrabutylammonium Bromide. *Talanta* **2000**, *53*, 645–650.
- (46) Tong, A.; Wu, Y.; Tan, S.; Li, L.; Akama, Y.; Tanaka, S. Aqueous Two-Phase System of Cationic and Anionic Surfactant Mixture and Its Application to the Extraction of Porphyrins and Metalloporphyrins. *Anal. Chim. Acta* **1998**, *369*, 11–16.
- (47) Yacilla, M. T.; Herrington, K. L.; Brasher, L. L.; Kaler, E. W.; Chiruvolu, S.; Zasadzinski, J. A. Phase Behavior of Aqueous Mixtures

of Cetyltrimethylammonium Bromide (CTAB) and Sodium Octyl Sulfate (SOS). *J. Phys. Chem.* **1996**, *100*, 5874–5879.

(48) Wilkins, M. H. F.; Blaurock, A. E.; Engelman, D. M. Bilayer Structure in Membranes. *Nature New Biol.* **1971**, *230*, 72–76.

(49) Alberty, R. A.; Massey, V. On the Interpretation of the PH Variation of the Maximum Initial Velocity of an Enzymecatalyzed Reaction. *Biochim. Biophys. Acta* **1954**, *13*, 347–353.

(50) Aledo, J. C.; Jiménez-Riveres, S.; Tena, M. The Effect of Temperature on the Enzyme-Catalyzed Reaction: Insights from Thermodynamics. *J. Chem. Educ.* **2010**, *87*, 296–298.

(51) Biosca, J. A.; Travers, F.; Hillaire, D.; Barman, T. E. Cryoenzymic Studies on Myosin Subfragment 1: Perturbation of an Enzyme Reaction by Temperature and Solvent. *Biochemistry* **1984**, *23*, 1947–1955.